ADVANCED MATERIALS
www.advmat.de

ADVANCED SCIENCE NEWS
www.advancedsciencenews.com

# High Temperature-Stable Perovskite Solar Cell Based on Low-Cost Carbon Nanotube Hole Contact

*Kerttu Aitola,* Konrad Domanski, Juan-Pablo Correa-Baena,* Kári Sveinbjörnsson, Michael Saliba, Antonio Abate, Michael Grätzel, Esko Kauppinen, Erik M. J. Johansson, Wolfgang Tress, Anders Hagfeldt, and Gerrit Boschloo*

**Mixed ion perovskite solar cells (PSC) are manufactured with a metal-free hole contact based on press-transferred single-walled carbon nanotube (SWCNT) film infiltrated with 2,2,7,-7-tetrakis(N,N-di-p-methoxyphenylamine)-9,90-spirobifluorene (Spiro-OMeTAD). By means of maximum power point tracking, their stabilities are compared with those of standard PSCs employing spin-coated Spiro-OMeTAD and a thermally evaporated Au back contact, under full 1 sun illumination, at 60 °C, and in a $N_2$ atmosphere. During the 140 h experiment, the solar cells with the Au electrode experience a dramatic, irreversible efficiency loss, rendering them effectively nonoperational, whereas the SWCNT-contacted devices show only a small linear efficiency loss with an extrapolated lifetime of 580 h.**

Perovskite solar cells[1] (PSCs) are a relatively new type of photovoltaic devices, which are based on light absorbing materials with the general formula of $ABX_3$, where A is a monovalent cation (methylammonium (MA), formamidinium (FA), Cs, or Rb), B is Pb or Sn, and X is a halide.[2–4] PSCs have recently attracted a lot of attention, owing to their very high power conversion efficiency (PCE; up to 22.1%),[5] cheap starting materials, and ease of fabrication. However, their poor stability, which has been linked to the sensitivity of the organometallic absorber toward humidity,[6] and their overall poor long-term thermal stability[7] have been the major factors hindering their fast commercialization. It has been proposed that the Cs-containing "triple cation" perovskites of the form Cs/FA/MA are structurally more stable than the $MAPbI_3$ and the mixed ion $FAPbI_3$:$MAPbBr_3$[8] perovskites, due to the smaller ionic radius of the Cs than those of the FA and MA cations.[3] This approach has been further advanced by the incorporation of Rb into the mixture to form the so-called "quadruple cation" PSCs.[2]

We have previously reported a crucial instability factor in PSCs operating at elevated temperatures related to Au from the back hole contact (HC) migrating through the entire solar cell structure and interacting with the perovskite, causing dramatic loss of solar cell performance.[9] Although the Au migration could be circumvented via the use of Cr interlayer between the Au contact and the hole transporting material (HTM; 2,2,7,7-tetrakis(*N,N*-di-*p*-methoxyphenylamine)-9,90-spirobifluorene, Spiro-OMeTAD), this came at the expense of a considerable efficiency decrease. In a subsequent work, we have shown that the problem of Au migration can be also circumvented by substituting Spiro-OMeTAD with the poly(triaryl amine) (PTAA) HTM.[2] However, this approach still involves the use of expensive Au contacts, and the PTAA polymer is currently also considerably more costly than the Spiro-OMeTAD HTM.

Different carbon-based alternative materials have been introduced as HTMs and HCs, such as carbon nanotube films with[10–12] and without[13] additional metal layers and carbon black composite contacts.[14,15] In our previous study, we demonstrated that a potentially cost-effective single-walled carbon nanotube (SWCNT) film deposited directly onto the $FAPbI_3$:$MAPbBr_3$ perovskite layer and processed further with a small amount of drop-cast Spiro-OMeTAD yielded high solar cell efficiencies of around 15%.[16] SWCNT-based contacts offer also other important advantages, such as extremely high flexibility[17] (which is a prerequisite for industrial roll-to-roll

Dr. K. Aitola, K. Sveinbjörnsson,
Prof. E. M. J. Johansson, Prof. G. Boschloo
Department of Chemistry – Ångström Laboratory
Physical Chemistry
Uppsala University
Box 523, 75120 Uppsala, Sweden
E-mail: kerttu.aitola@kemi.uu.se

K. Domanski, Dr. M. Saliba, Prof. M. Grätzel, Dr. W. Tress
Laboratory for Photonics and Interfaces
Institute of Chemical Sciences and Engineering
École Polytechnique de Fédérale de Lausanne
CH-1015 Lausanne, Switzerland

Dr. J.-P. Correa-Baena
Massachusetts Institute of Technology
77 Massachusetts Avenue, Cambridge, MA 02139, USA
E-mail: jpcorrea@mit.edu

Dr. A. Abate
Adolphe Merkle Institute
University of Fribourg
CH-1700 Fribourg, Switzerland

Prof. E. Kauppinen
Department of Applied Physics
Aalto University
P.O. Box 15100, 00076 Aalto, Finland

Prof. A. Hagfeldt
Laboratory of Photomolecular Science
Institute of Chemical Sciences and Engineering
École Polytechnique Fédérale de Lausanne
CH-1015 Lausanne, Switzerland

DOI: 10.1002/adma.201606398

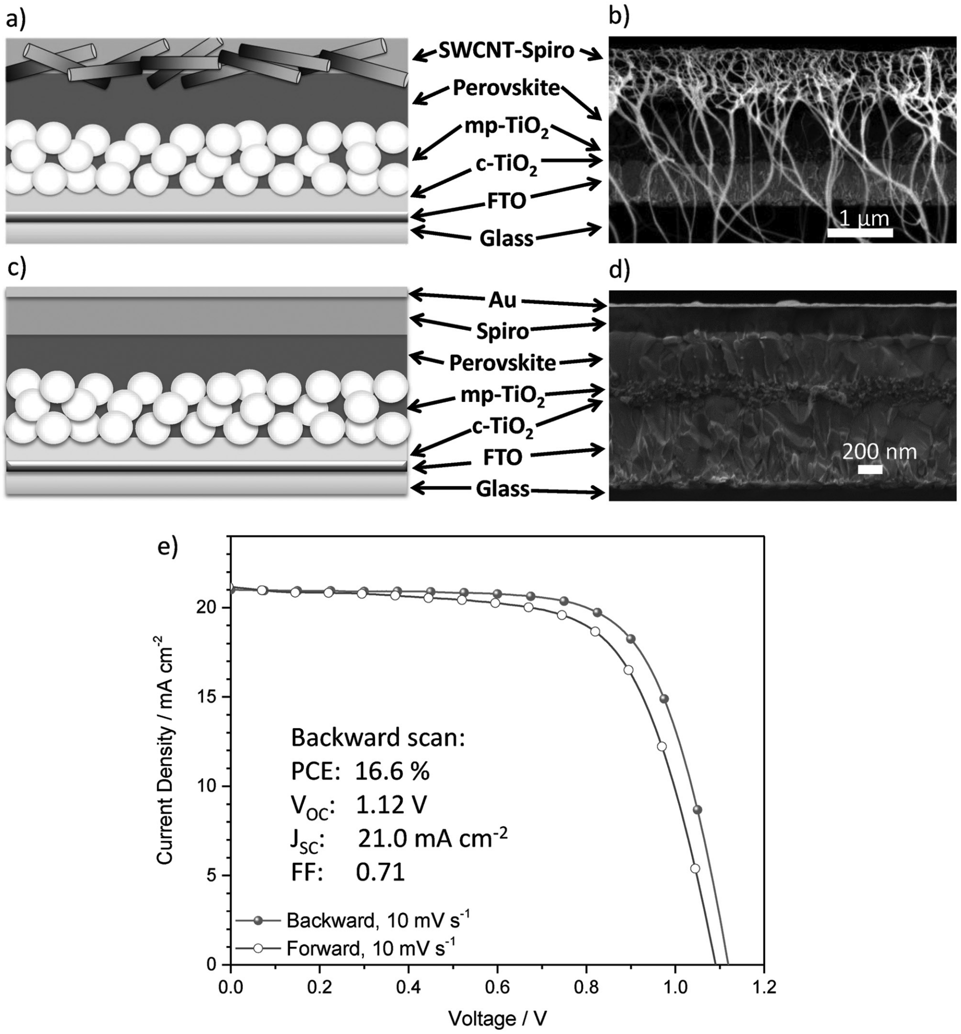

**Figure 1.** a) Schematics and b) cross-sectional SEM image of the SWCNT-contacted device. The carbon nanotube “whiskers” in front of the SEM image are due to sample preparation. c) Schematics and d) cross-sectional SEM image of the standard Au contacted device (with spin-coated Spiro-OMeTAD HTM. e) The *J–V* curve of a device that yielded a 16.0% average efficiency (average of the backward and forward scans).

deposition processes) and semitransparency,[18] which is required in, e.g., bifacial solar cells. Snaith and co-workers have also suggested that a SWCNT-poly(methyl methacrylate) (PMMA) composite may protect the perovskite films from ambient humidity even more efficiently than PMMA alone due to the hydrophobic nature of SWCNTs.[11]

In this work, we show that PSCs employing a SWCNT-based HTM-HC have superior long-term stability at elevated temperatures (60 °C—temperature commonly used for solar cell stability testing[19]), as compared to that of the standard configuration with an evaporated Au contact with Spiro-OMETAD HTM. We fabricated devices based on fluorine-doped tin oxide (FTO)/compact TiO$_2$/mesoporous TiO$_2$/perovskite/Spiro-OMeTAD/HC architecture, with $Cs_5(MA_{0.17}FA_{0.83})_{95}Pb(I_{0.83}Br_{0.17})_3$ perovskite as the active layer (from here on referred to as “mixed ion perovskite”). Two types of HTM-HC configurations were used: (1) spin-coated Spiro-OMeTAD and evaporated Au contact and (2) SWCNT:Spiro-OMeTAD composite HTM-HC[16] manufactured by a simple press transfer of the SWCNT film on the perovskite layer and infiltrating the SWCNT film with Spiro-OMeTAD (i.e., no additional Au or Ag contact or a separate Spiro-OMeTAD layer is utilized in the structure; the latter configuration is depicted in **Figure 1**a,b and the standard one in Figure 1c,d).

In this study, both the short-circuit current density ($J_{SC}$) and the open circuit voltage ($V_{OC}$) were, on average, similar for the both types of cells (cf. Figures 1c and 3a,b). While the similar $V_{OC}$ is in line with our previous findings,[16] we note no mismatch in $J_{SC}$s of the Au and SWCNT contacted devices, as we did in the previous study (where the $J_{SC}$ was lower for the SWCNT devices as compared to the Au devices). In this work, the currents for the SWCNT devices are overall a bit higher (21–22 mA cm$^{-2}$) than in the previous study (≈20 mA cm$^{-2}$). This suggests that in the currently used perovskite films’ case, the film absorbs most of the incoming light and Au back reflection does not contribute to the current generation. This is due to the thicker perovskite film (500 nm)[20] compared to what was used in our previous work (300–400 nm).[16] Finally, the relatively lower fill factor (FF) in the SWCNT devices (compared to spin-coated Spiro-OMeTAD-perovskite interface) is most likely related to the somewhat unoptimized contact between the SWCNT-Spiro-OMeTAD composite and the perovskite layer.[16] The higher sheet resistance of the SWCNT-Spiro-OMeTAD composite film ($\approx 15\ \Omega\ \square^{-1}$ compared to $<1\ \Omega\ \square^{-1}$ for Au layer) further reduces the FF. Nevertheless, high efficiency (>16%) PSCs can be manufactured with the SWCNT-based HTM-HC, without the use of costly metal electrodes.

The results from the 140 h maximum power point (MPP) tracking of the Au and SWCNT-contacted devices under white light-emitting diode (LED) illumination with an intensity equivalent to 1 sun, carried out in $N_2$ atmosphere, can be seen in **Figure 2**. A Au-contacted device yielding a PCE of 18.4% (18.0% stabilized) and a SWCNT device yielding 15.0% PCE (14.3% stabilized) were used in the stability testing. The lower performance of the latter, as compared to the device in Figure 1c, was due to its slightly lower $V_{OC}$ (1.03 V) and FF (0.63). The cells were kept at the temperature of 20 °C for the first 14 h of the ageing experiment, and one can see that the Au-contacted device has shown pronounced changes within this period. We added also results from a 90 h MPP tracking of an Au device conducted in 20 °C in Figure 2a to highlight the initial degradation of PSCs in lower temperatures, followed by a stabilization period, which is not seen in high temperature experiments, where Au devices undergo an irreversible degradation process. We have previously shown that the changes occurring in 20 °C experiments are due to slow cation migration in the devices happening in the timescale of hours and they are mostly of reversible nature and the cells recover most of their performance if they are allowed to relax 7–8 h in the dark.[9,21] Curiously, the SWCNT device exhibits only a small efficiency drop in this region. According to our practical experience, this initial efficiency loss phenomenon is not usually so pronounced for lower efficiency (<18%) solar cells, like the SWCNT cells, and we believe that in the lower efficiency cells' case it is masked by for instance initially higher series resistances.

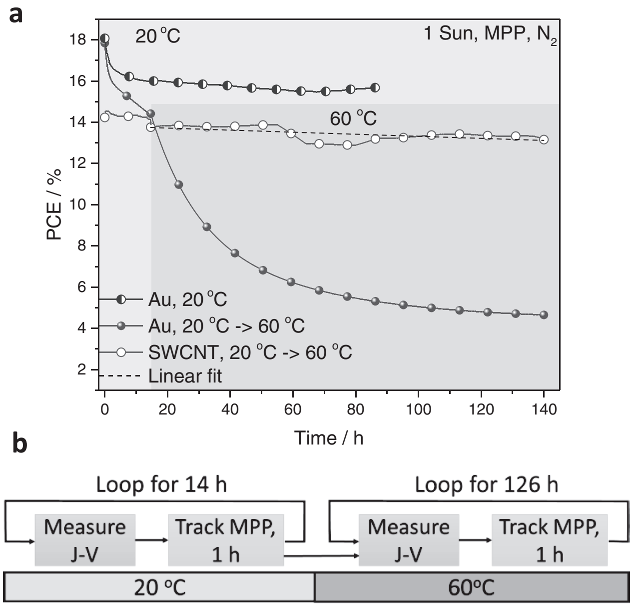

**Figure 2.** a) The result of MPP tracking of Au and SWCNT-contacted devices at elevated temperatures. b) The temperature of the devices was changed from initial 20 to 60 °C after 14 h into the experiment. MPP tracking of an Au device at 20 °C is shown for 90 h.

After the temperature was increased to 60 °C, the degradation of the Au-based device accelerated dramatically. The device showed an exponential decay, losing 20% of the remaining PCE within only 8 h of ageing. This is expected and has been shown by us to be due to Au migration-induced degradation of the device.[9] In contrast, the SWCNT-contacted device showed a slow decay which can be approximated with a linear function yielding a slope of $-0.005\%\ h^{-1}$. Assuming that this trend continues, we extrapolate a very conservative estimate of the predicted lifetime (defined as the point, where 20% of initial PCE is lost, T80) of 580 h. With a simplistic assumption that the degradation rate is directly proportional to the light intensity, this value corresponds to half a year of operation given an average of three sun shine hours a day—typical value for central Europe.[22]

We further investigated the nature of degradation of the two devices by tracking the evolution of the *J*–*V* curves and the *J*–*V* metrics over the course of the ageing experiment (**Figure 3**). The Au-based device degraded significantly including a significant worsening of all the main *J*–*V* parameters. Notably, the considerable loss of $V_{OC}$ has been previously demonstrated to be an indication of Au-induced degradation of the perovskite layer.[9] Importantly, the SWCNT device showed only a minor decrease in $V_{OC}$ and $J_{SC}$, which could be due to, e.g., perovskite phase transition, slow degradation due to residual water or oxygen in the perovskite film, light induced trap states or ionic movement—degradation mechanisms of perovskite films employed in photovoltaic devices are not well known yet thus all the aforementioned reasons are so far only speculative. However, our work shows that a carbon nanotube film, deposited by simple nonvacuum means and with the use of which the metal migration issue can be avoided completely, is a promising option for hole contact in stable PSCs.

In this work, we have shown that perovskite solar cells employing a mixed ion perovskite absorber and a single-walled carbon nanotube-based hole-transporting material and hole contact are good candidates for durable and efficient photovoltaic devices. During the experiment conducted at 60 °C in $N_2$ atmosphere and 1 sun equivalent white LED illumination, the devices showed only a modest linear efficiency loss (slope: $-0.005\%\ h^{-1}$), which led to an estimated lifetime (T80) of 580 h. At the same time, the standard PCSs with a Au back contact experienced a dramatic and rapid efficiency loss; likely due to the Au ion migration in the structure.

## Experimental Section

*SWCNT Synthesis*: The SWCNTs were synthesized by a floating catalyst-chemical vapor deposition procedure described in ref. [18]. Shortly, ferrocene containing CO:$CO_2$ (99:1 ratio) carrier gas was directed into a hot furnace reactor kept at 880 °C. The ferrocene decomposed in the temperature gradient between the gas injector and the reactor forming catalytic iron nanoparticles, that acted as catalysts for the CO:$CO_2$ gas decomposition and SWCNTs started forming on the nanoparticles. The formed SWCNTs were collected from the gas phase

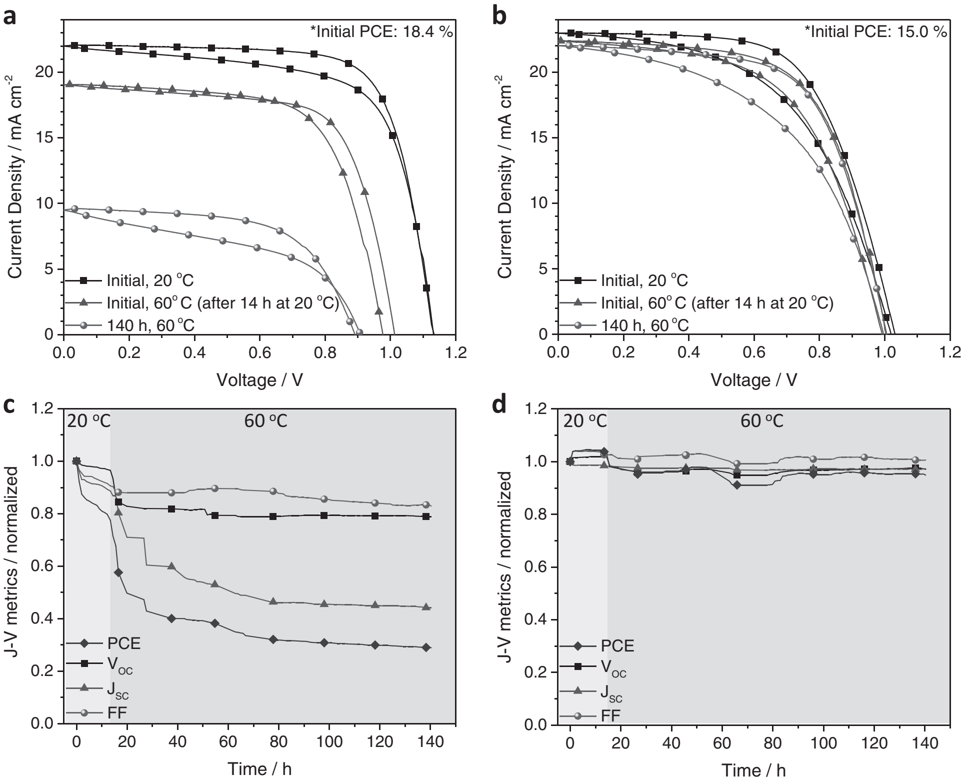

**Figure 3.** *J*–*V* curves of a) Au and b) SWCNT-contacted devices at the beginning of the experiment at 20 °C, at 60 °C after the temperature increase, and at the end of the experiment (at 60 °C). c,d) The evolution of individual *J*–*V* metrics (PCE, $V_{OC}$, $J_{SC}$, and FF) over the course of the experiment.

on a porous filter membrane at the reactor outlet and the formed film could be transferred from the filter paper on the desired substrate.

*Fabrication of Perovskite Solar Cells*: FTO glass sheets (Nippon Sheet Glass 10) were etched with zinc powder and HCl (4 M). Substrates were ultrasonically cleaned by a sequential 15 min 2% Hellmanex water solution, deionized water, ethanol, and acetone. Substrates were treated under UV-ozone for 15 min to remove the last traces of organic residues. A 30–50 nm thin compact $TiO_2$ layer was then deposited on to the clean preheated substrates by spray pyrolysis from a precursor solution of titanium diisopropoxide bis(acetylacetonate) in anhydrous ethanol, using oxygen as the carrier gas on a hot plate set to 450 °C, followed by annealing at 450 °C, for 30 min in air. A mesoporous $TiO_2$ layer was deposited by spin coating for 20 s at 4000 rpm with a ramp of 2000 rpm, using 30 nm particle paste (Dyesol 30 NR-D) diluted in ethanol to achieve a 200 nm layer thickness (150 mg mL$^{-1}$). After the spin coating, the substrates were immediately dried at 100 °C for 10 min and then sintered again at 450 °C for 30 min under dry air flow.

Li-doping of mesoporous $TiO_2$[23] was accomplished by spin coating a 0.1 M solution of Li-TFSI in acetonitrile at 3000 rpm with a ramp of 1000 rpm for 10 s, followed by another sintering step at 450 °C for 30 min. After cooling down to 150 °C, the substrates were immediately transferred to a nitrogen atmosphere glove box for depositing the perovskite films.

The mixed triple-cation lead mixed-halide perovskite solution was prepared from a precursor solution made of formamidinium iodide (FAI) (1 M, Dyesol), $PbI_2$ (1.1 M, TCI), MABr (0.2 M, Dyesol), and $PbBr_2$ (0.22 M, TCI) in a 4:1 (V:V) mixture of anhydrous dimethylformamide:dimethylsulfoxide (DMSO) (Acros). Then, a 1.5 M stock solution of CsI (abcr GmbH) in DMSO was added to the above solution in 5:95 volume ratio. The mixed ion perovskite solution was deposited through a two-step spin coating program (10 s at 1000 rpm and 20 s at 6000 rpm). During the second step, 200 µL of chlorobenzene was poured on the spinning substrate 5 s before the end of the procedure. The substrates were then placed on a hotplate for annealing at 100 °C for 1 h in a nitrogen filled glove box.

After the perovskite annealing, the substrates were cooled down for a few minutes and a Spiro-OMeTAD (Merck) solution (70 × 10$^{-3}$ M in chlorobenzene) was spin coated at 4000 rpm for 20 s. Spiro-OMeTAD was doped with bis(trifluoromethylsulphonyl)imide lithium salt (Li-TFSI, Sigma-Aldrich), tris(2-(1H-pyrazol-1-yl)-4-*tert*-butylpyridine)cobalt(III) tris(bis(trifluoromethyl-sulphonyl)imide) (FK209, Dyenamo), and 4-*tert*-butylpyridine (TBP, Sigma-Aldrich). The molar ratio of additives for Spiro-OMeTAD was 0.5, 0.03, and 3.3 for Li-TFSI, FK209, and TBP, respectively.

In the reference "standard" solar cells case, an 80 nm thick gold top electrode was deposited on the Spiro-OMeTAD layer as top contact electrode by thermal evaporation under high vacuum.

The SWCNT solar cells were prepared by cutting the SWCNT film on filter paper to around 5 mm × 10 mm size piece and transferred on the perovskite substrate using some pressure, after which the filter paper was peeled off the SWCNT film. The SWCNT film was "densified"[18] with a small amount of chlorobenzene. After that another SWCNT film was transferred on the first film in order to reach lower sheet resistance than with the single film layer.[16] Finally, 2 × 2 µL drops of Spiro-OMeTAD solution were drop cast on the SWCNT film.

*J*–*V Measurements: J*–*V* measurements were performed with a Newport Solar Simulator, model 91160, equipped with a Keithley 2400 source meter, and providing a 1000 W m$^{-2}$ AM 1.5G illumination intensity, as measured by means of a certified reference silicon solar cell (Fraunhofer - Institut für Solare Energiesysteme ISE). A slow (10 mV s$^{-1}$) scan speed was used in the initial *J*–*V* measurements.

*Stability Measurements*: Stability measurements were performed with a Biologic MPG2 potentiostat under white LED lamp (Lumileds LXM3-PW51) with 1 sun equivalent intensity. The devices were masked

(0.16 cm$^2$) and flushed with nitrogen for several hours before the start of the experiment in order to remove residual oxygen and water from the environment of an in-house developed sample holder. Then, the *J–V* curves of the devices were measured at 100 mV s$^{-1}$ (high scan speed was chosen to maximize the time that the devices spend at MPP) followed by MPP tracking routine under continuous illumination (and $N_2$). The MPP was updated every 10 s by a standard perturb and observe method and continued for 1 h before the procedure was repeated starting with measuring the *J–V* curve again. The temperature of the devices was controlled with a Peltier element in direct contact with the films. The temperature was measured with a surface thermometer located between the Peltier element and the film. While the initial temperature was set to 20 °C, it was changed to 60 °C after 14 h into the experiment without disturbing the ongoing data collection. The temperature equilibration time was below 1 min. All devices were tested at the same time inside one sample holder—hence being exposed to identical environmental conditions: temperature, illumination, and atmosphere.

*Electron Microscopy Analysis*: Scanning electron microscopy (SEM) characterization of the device stack was performed with a ZEISS Merlin high resolution SEM.

## Acknowledgements

K.A. and K.D. contributed equally to this work. K.A. is grateful for the Wallenberg foundation, Swedish Research Council FORMAS, Swedish Energy Agency and the Solar-era.net project "CNT-PV" for the financial support. K.D. thanks the Fonds national suisse for funding within the framework of Umbrella project (Grant Agreement Nos. 407040-153952 and 407040-153990). We thank Benjamin Le Geyt, Supardi Sujito, Christophe Clement and Andre Fattet for their help in setting up infrastructure used for this work.

Received: November 25, 2016

---

[1] M. M. Lee, J. Teuscher, T. Miyasaka, T. N. Murakami, H. J. Snaith, *Science* **2012**, *338*, 643.
[2] M. Saliba, T. Matsui, K. Domanski, J.-Y. Seo, A. Ummadisingu, S. M. Zakeeruddin, J.-P. Correa-Baena, W. R. Tress, A. Abate, A. Hagfeldt, M. Gratzel, *Science* **2016**, *354*, 206.
[3] M. Saliba, T. Matsui, J.-Y. Seo, K. Domanski, J.-P. Correa-Baena, M. K. Nazeeruddin, S. M. Zakeeruddin, W. Tress, A. Abate, A. Hagfeldt, M. Grätzel, *Energy Environ. Sci.* **2016**, *9*, 1989.
[4] N. J. Jeon, J. H. Noh, Y. C. Kim, W. S. Yang, S. Ryu, S. Il Seok, *Nat. Mater.* **2014**, *13*, 1.
[5] NREL Best Research Cell Efficiencies, http://www.nrel.gov/pv/assets/images/efficiency-chart.png, (accessed: January 2017).
[6] J. Yang, B. D. Siempelkamp, D. Liu, T. L. Kelly, *ACS Nano* **2015**, *9*, 1955.
[7] B. Conings, J. Drijkoningen, N. Gauquelin, A. Babayigit, J. D'Haen, L. D'Olieslaeger, A. Ethirajan, J. Verbeeck, J. Manca, E. Mosconi, F. De Angelis, H.-G. Boyen, *Adv. Energy Mater.* **2015**, *5*, 1500477.
[8] N. J. Jeon, J. H. Noh, W. S. Yang, Y. C. Kim, S. Ryu, J. Seo, I. Sang, *Nature* **2015**, *517*, 476.
[9] K. Domanski, J.-P. Correa-Baena, N. Mine, M. K. Nazeeruddin, A. Abate, M. Saliba, W. Tress, A. Hagfeldt, M. Grätzel, *ACS Nano* **2016**, *10*, 6306.
[10] S. N. Habisreutinger, T. Leijtens, G. E. Eperon, S. D. Stranks, R. J. Nicholas, H. J. Snaith, *J. Phys. Chem. Lett.* **2014**, *5*, 4207.
[11] S. N. Habisreutinger, T. Leijtens, G. E. Eperon, S. D. Stranks, R. J. Nicholas, H. J. Snaith, *Nano Lett.* **2014**, *14*, 5561.
[12] R. Ihly, A.-M. Dowgiallo, M. Yang, P. Schulz, N. Stanton, O. G. Reid, A. Ferguson, K. Zhu, J. J. Berry, J. Blackburn, *Energy Environ. Sci.* **2016**, *9*, 1439.
[13] Z. Li, S. A. Kulkarni, P. P. Boix, E. Shi, A. Cao, K. Fu, S. K. Batabyal, J. Zhang, Q. Xiong, L. H. Wong, N. Mathews, S. G. Mhaisalkar, *ACS Nano* **2014**, *8*, 6797.
[14] A. Mei, X. Li, L. Liu, Z. Ku, T. Liu, Y. Rong, M. Xu, M. Hu, J. Chen, Y. Yang, M. Grätzel, H. Han, *Science* **2014**, *345*, 295.
[15] H. Zhou, Y. Shi, Q. Dong, H. Zhang, Y. Xing, K. Wang, Y. Du, T. Ma, *J. Phys. Chem. Lett.* **2014**, *5*, 3241.
[16] K. Aitola, K. Sveinbjörnsson, J. P. Correa Baena, A. Kaskela, A. Abate, Y. Tian, E. M. J. Johansson, M. Grätzel, E. Kauppinen, A. Hagfeldt, G. Boschloo, *Energy Environ. Sci.* **2016**, *9*, 461.
[17] N. Saran, K. Parikh, D.-S. Suh, E. Muñoz, H. Kolla, S. K. Manohar, *J. Am. Chem. Soc.* **2004**, *126*, 4462.
[18] A. Kaskela, A. G. Nasibulin, M. Y. Timmermans, B. Aitchison, A. Papadimitratos, Y. Tian, Z. Zhu, H. Jiang, D. P. Brown, A. Zakhidov, E. I. Kauppinen, *Nano Lett.* **2010**, *10*, 4349.
[19] M. O. Reese, S. A. Gevorgyan, M. Jørgensen, E. Bundgaard, S. R. Kurtz, D. S. Ginley, D. C. Olson, M. T. Lloyd, P. Morvillo, E. A. Katz, A. Elschner, O. Haillant, T. R. Currier, V. Shrotriya, M. Hermenau, M. Riede, K. R. Kirov, G. Trimmel, T. Rath, O. Inganäs, F. Zhang, M. Andersson, K. Tvingstedt, M. Lira-Cantu, D. Laird, C. McGuiness, S. Gowrisanker, M. Pannone, M. Xiao, J. Hauch, R. Steim, D. M. Delongchamp, R. Rösch, H. Hoppe, N. Espinosa, A. Urbina, G. Yaman-Uzunoglu, J.-B. Bonekamp, A. J. J. M. Van Breemen, C. Girotto, E. Voroshazi, F. C. Krebs, *Sol. Energy Mater. Sol. Cells* **2011**, *95*, 1253.
[20] J. P. Correa-Baena, M. Anaya, G. Lozano, W. Tress, K. Domanski, M. Saliba, T. Matsui, T. J. Jacobsson, M. E. Calvo, A. Abate, M. Grätzel, H. Míguez, A. Hagfeldt, *Adv. Mater.* **2016**, *1*, 5031.
[21] E. H. Anaraki, A. Kermanpur, L. Steier, K. Domanski, T. Matsui, W. Tress, M. Saliba, A. Abate, M. Grätzel, A. Hagfeldt, J.-P. Correa-Baena, *Energy Environ. Sci.* **2016**, *9*, 3128.
[22] PVWatts Calculator, http://pvwatts.nrel.gov/, n.d (accessed: 18 August 2016).
[23] F. Giordano, A. Abate, J. Pablo, C. Baena, M. Saliba, T. Matsui, S. H. Im, S. M. Zakeeruddin, M. K. Nazeeruddin, A. Hagfeldt, M. Graetzel, *Nat. Commun.* **2016**, *7*, 1.